Hydraulic Control of Flows with Nonuniform Potential Vorticity*

LAWRENCE J. PRATT

Woods Hole Oceanographic Institution, Woods Hole, MA 02543

LAURENCE ARMI

Scripps Institution of Oceanography, La Jolla, CA 92093

(Manuscript received 5 March 1987, in final form 26 May 1987)

ABSTRACT

The hydraulics of flow contained in a channel and having nonuniform potential vorticity is considered from a general standpoint. The channel cross section is rectangular and the potential vorticity is assumed to be prescribed in terms of the streamfunction. We show that the general computational problem can be expressed in two traditional forms, the first of which consists of an algebraic relation between the channel geometry and a single dependent flow variable and the second of which consists of a pair of quasi-linear differential equations relating the geometry to two dependent flow variables. From these forms we derive a general "branch condition" indicating a merger of different solutions having the same flow rate and energy and show that this condition implies that the flow is critical with respect to a certain long wave. It is shown that critical flow can occur only at the sill in a channel of constant width (with one exception) at a point of width extremum in a flat bottom channel. We also discuss the situation in which the fluid becomes detached from one of the sidewalls.

An example is given in which the potential vorticity is a linear function of the streamfunction and the rotation rate is zero, a case which can be solved analytically. When the potential vorticity gradient points downstream, allowing propagation of potential vorticity waves against the flow, multiple pairs of steady states are possible, each having a unique modal structure. Critical control of the higher-mode solutions is primarily over vorticity, rather than depth. Flow reversals arise in some situations, possibly invalidating the prescription of potential vorticity.

1. Introduction

Over the past 15 years there have been a number of investigations of hydraulically driven flow in rotating channels emphasizing the pertinence of classical hydraulics concepts such as critical control. These studies have been directed towards reaching a better understanding of the dynamics of deep strait and sill flow in the ocean. Adrian Gill was one of the leaders in this field and his 1977 paper not only advanced the state of knowledge (by extending the theory for zero potential vorticity flow to finite but uniform potential vorticity) but also presented a unifying approach which illuminated various aspects of hydraulics problems in general. His work clarified earlier results by Whitehead et al. (1974) and Sambuco and Whitehead (1976) and laid much of the groundwork for later advancements (e.g., Roed, 1980; Shen, 1981; Pratt, 1983, 1984a; Hogg, 1983, 1985; Borenäs and Lundberg, 1986). If one were forced to choose from among all hydraulics papers ever written one which most clearly describes the concepts of hydraulic control, supercritical and subcritical flow, and solution branch points, one could not go far wrong choosing Gill's (1977) work.

"Hydraulics" and "hydraulic control" have always been loosely defined terms and one of the few attempts at a definition is due to Gill. According to his definition one must be able to describe the flow in terms of a single dependent variable [say $d(x)$] which can be expressed in terms of the slowly varying geometric parameters of the channel (the width $w(x)$, the bottom elevation $h(x)$, etc.) by a relationship of the form

$$\mathcal{F}[d(x); w(x), h(x), \cdots] = \text{constant}. \tag{1.1}$$

The relationship must be multivalued in that d may take on several values for given w, h, etc. Under these circumstances the condition

$$\partial\mathcal{F}/\partial d = 0 \tag{1.2}$$

indicates a merging of the different solution branches or roots. Since the function $\mathcal{F}$ does not depend explicitly on position x, the solutions possess a kind of symmetry with respect to the channel geometry and the flow field will be identical at any two sections having the same w, h, etc. The only exception occurs when the solution passes through a branch point between the two sections, in which case symmetry is lost. Since

* Woods Hole Oceanographic Institution Contribution No. 6479.

$$d\mathcal{J}/dx = \frac{\partial \mathcal{J}}{\partial d}\frac{d(d)}{dx} + \frac{\partial \mathcal{J}}{\partial w}\frac{dw}{dx} + \frac{\partial \mathcal{J}}{\partial h}\frac{dh}{dx} + \cdots = 0, \quad (1.3)$$

the branch or control point must lie at a topographic extremum, that is where

$$\frac{\partial \mathcal{J}}{\partial w}\frac{dw}{dx} + \frac{\partial \mathcal{J}}{\partial h}\frac{dh}{dx} + \cdots = 0$$

in view of (1.2). For the special case of uniform, finite potential vorticity Gill (1977) constructs the function $\mathcal{J}$ and shows that the condition (1.2) is equivalent to the condition that long waves (in this case Kelvin waves) become stationary in the flow. The steady flow is therefore critical at a branch point and information which exists downstream is not felt upstream of this section. Such a flow is said to be hydraulically controlled and can be computed by starting at the control section and working one's way upstream and downstream.

Another view of "hydraulics type" problems is based on one's ability to express the problem in the quasi-linear form

$$\mathbf{C}\mathbf{d}_x = \mathbf{D}\mathbf{f}_x, \quad (1.4)$$

where **d** and **f** are vectors containing the dependent flow variables and forcing terms (including topographic forcing) respectively, and the coefficient matrices **C** and **D** depend on the dependent and independent variables, but not derivatives of the dependent variables. The eigenvalue problem for (1.4), $\mathrm{Det}(\mathbf{C} - \lambda\mathbf{I}) = 0$, gives the critical condition for long waves when $\lambda = 0$. The consequential restriction on the forcing term **f** follows directly from (1.4). In the study of the hydraulics of multiple density layer flows (e.g., Armi, 1986) it is common to use (1.4) as a starting point.

Although (1.4) can often be integrated and the result manipulated to achieve a relationship of the form (1.1), this is not always the case. For example, in Pratt's (1986) study of hydraulically driven flow with bottom drag, equations of the form (1.4) are found; however, when these equations are integrated the function $\mathcal{J}$ is found to contain explicit dependence on x. Also, weakly dispersive, hydraulically driven flow in rotating channels exhibits many classical hydraulics features and yet cannot be described in either form (Pratt, 1984a).

This paper explores the important but mathematically difficult problem of computing hydraulically driven channel flows having nonuniform potential vorticity. To simplify the problem as much as possible, we consider a channel of rectangular cross section extending from a reservoir or basin in which the potential vorticity is known along each streamline. One of the complications introduced by potential vorticity nonuniformity is an additional restoring mechanism associated with the potential vorticity gradient. Thus, we expect that many long-wave modes of the mixed potential vorticity–gravity type will arise and that multiple critical states may exist in the steady solutions. Analogies exist in stratified fluids, where the flow may become critical with respect to various internal modes (Farmer and Denton, 1985) and in coastal currents, where criticalities may exist with respect to Kelvin and shelf modes (Hughes, 1985, 1987).

There are a number of reasons for considering nonuniform potential vorticity distributions. The main one, of course, is that the complicated processes involved in the formation of overflow water will, in general, lead to complicated potential vorticity distributions. Even if the newly formed overflow water has uniform potential vorticity, significant nonuniformities may develop due to friction by the time the fluid reaches the sill. (Pratt, 1986, has argued that bottom friction can be particularly significant in the major deep-sea overflows). Finally, there are other current systems which may experience upstream effects associated with potential vorticity waves: the Gulf Stream, the Kuroshio, and the Antarctic Circumpolar Current are three possibilities. Although the boundary conditions of the present model are not particularly relevant to these currents, common dynamical features may exist.

Our immediate task is to show that the hydraulics problem with nonuniform, but prescribed, potential vorticity can be cast in the two traditional forms (1.1) and (1.4). The purpose of this is twofold; first, it provides a framework for the computation of such flows by presenting equations which could be used as the basis for a numerical algorithm. More importantly, it allows us to deduce a number of facts concerning the symmetry of the flow and the location and physical nature of points of hydraulic control. In section 2 we show how the hydraulics problem can be put in the forms (1.1) and (1.4) and derive a general criterion for Gill's branch point condition (1.3). In this somewhat abstract discussion the flow field is represented at a given cross section by two independent quantities $C_1(x)$ and $C_2(x)$ which the investigator is free to choose in a variety of ways. The patient reader will find some relief in the form of physical intuition in sections 3 and 4, where $C_1(x)$ and $C_2(x)$ are chosen to be the average and difference, respectively, of the fluid depths along the channel walls. This choice allows the flow at a branch point to be discussed in clearer physical terms and we show, in particular, that the sidewall specific energies are stationary at such a point and that the flow is critical with respect to a long wave which does not disturb the basic potential vorticity. Also discussed are the geometrical restrictions on the channel which must be met in order for critical flow to occur. Finally, section 5 discusses the applicability of these ideas when the fluid is separated from one of the sidewalls.

The second half of the paper is devoted to examples which provide additional insight into the physics of this complex problem. Section 6 contains some short

examples of uniform potential vorticity flows illustrating the computational method, particularly the choice of $C_1(x)$ and $C_2(x)$, and showing that the method reproduces known results. Section 7 describes a much richer example in which the potential vorticity distribution is chosen so as to allow an analytical solution. Here we show that many pairs of (supercritical and subcritical) solutions can be found for the same flow rate, energy, and potential vorticity distribution. Each pair has a single branch point where the subcritical and supercritical solution branches meet and the flow is critical with respect to a mixed potential vorticity–gravity wave.

2. The equations for steady flow

Consider the steady shallow flow of homogeneous, inviscid fluid in the rotating channel of rectangular cross section shown in Fig. 1. The independent variables x and y denote distance along and perpendicular to the channel axis, the channel sidewalls lie at $y = \pm w(x)$, and the elevation of the bottom is $h(x)$. Also $d(x, y)$ and $[u(x, y), v(x, y)]$ denote the fluid depth and the x- and y-velocity components. If the channel width and bottom elevation vary on a scale large compared to w, it can be shown (e.g., Gill, 1977) that the flow is approximately governed by the semigeostrophic shallow water equations:

$$uu_x + vu_y - fv = -gd_x - gh_x \tag{2.1}$$

$$fu = -gd_y \tag{2.2}$$

$$(ud)_x + (vd)_y = 0, \tag{2.3}$$

where f is the Coriolis parameter and g is the gravitational acceleration. From these equations it can be shown that the semigeostrophic potential vorticity $(f - u_y)/d$ is conserved along streamlines:

$$(f - u_y)/d = G(\psi), \tag{2.4}$$

where the streamfunction ψ is defined by

$$\psi_x = vd \quad \psi_y = -ud. \tag{2.5a, b}$$

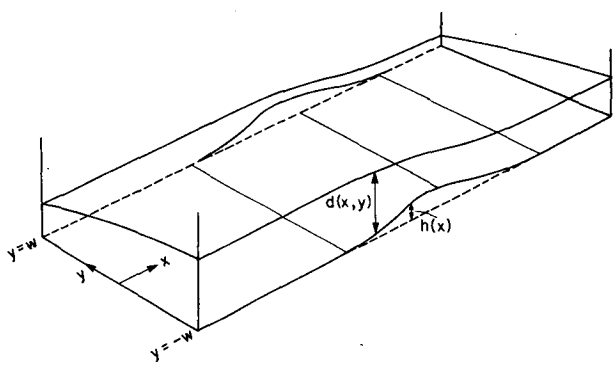

FIG. 1. Definition sketch.

Furthermore, it can be shown that the semigeostrophic Bernoulli function

$$\tfrac{1}{2}u^2 + gd + gh = B(\psi) \tag{2.6}$$

and the potential vorticity are related by

$$dB/d\psi = G(\psi). \tag{2.7}$$

The traditional approach to the rotating channel flow problem is to specify $G(\psi)$ at some section far upstream, usually in a very wide or deep reservoir, and then compute the flow downstream of this section by solving any three of (2.1)–(2.4) and (2.6) subject to the boundary conditions

$$v(x, w) = u(x, w)dw/dx \tag{2.8a}$$

$$v(x, -w) = -u(x, -w)dw/dx. \tag{2.8b}$$

It is also possible for the fluid to separate from one of the sidewalls, in which case a new boundary condition arises. This case will be taken up in section 5; for now discussion will be confined to the case of finite depth across the entire channel.

Previous investigations have been confined to the case G = constant; now consider the computation of the flow field for more general $G(\psi)$. Multiplying (2.2) by d and substituting (2.5b) for (ud) leads to the following relationship between ψ and d:

$$\psi = (g/2f)[d^2(x, y) - d^2(x, w)], \tag{2.9}$$

where the value of ψ has arbitrarily been chosen as zero along the wall at $y = w$. Substituting (2.9) into (2.4) and combining the result with (2.2) yields an equation for the cross-channel depth structure:

$$d_{yy} - fg^{-1}G[d^2 - d^2(x, w)]d + f^2g^{-1} = 0. \tag{2.10}$$

Since no derivatives with respect to x appear in (2.10), the variable x may be treated as a parameter. Thus the solution to the second-order equation will depend on two integration "constants": $C_1(x)$ and $C_2(x)$. It is possible to choose one of the "constants" as $d(x, w)$, or to make other physically convenient choices with no loss of generality; however, we will leave $C_1(x)$ and $C_2(x)$ undefined for the present. In summary

$$d = D[y; C_1(x), C_2(x)] \tag{2.11}$$

and, in view of (2.2):

$$u = -gf^{-1}D_y = U[y; C_1(x), C_2(x)]. \tag{2.12}$$

At this point there are a number of ways of constructing the function $\mathcal{F}$ required by Gill. One is to evaluate the Bernoulli equation (2.6) along each sidewall and use (2.7) to write the Bernoulli constant at $y = w$ in terms of its value at $y = -w$, resulting in

$$E^+(w, C_1, C_2) = -gh + B^- - \int_0^Q G(\hat{\psi})d\hat{\psi} \tag{2.13a}$$

$$E^-(-w, C_1, C_2) = -gh + B^-, \quad (2.13b)$$

where the superscripts "+" and "−" denote values at $y = w$ and $y = -w$, Q is the value of ψ at $y = -w$ (the flow rate), and

$$E^+ = \tfrac{1}{2}(U^+)^2 + gD^+ \quad (2.14a)$$

$$E^- = \tfrac{1}{2}(U^-)^2 + gD^- \quad (2.14b)$$

are the "specific energies" at $y = \pm w$. In principle, either (2.13a or b) determines C_2 in terms of C_1, w and h, and this relationship can be substituted into the other equation to obtain the desired $\mathcal{F}$-function. For example substitution into (2.13b) leads to

$$\mathcal{F}(C_1; w, h) = E^-[-w, C_1, C_2(C_1, w, h)] + gh = B^-, \quad (2.15)$$

and this relation establishes the symmetry relation mentioned earlier; a flow specified by B^-, Q and G will have identical structure (i.e., identical C_1, C_2) at any two sections of identical w and h, unless a branch point is passed in between.

The branch point condition $\partial\mathcal{F}/\partial C_1 = 0$ [see Eq. (1.2)] leads to

$$E_{C_1}^- + E_{C_2}^-(\partial C_2/\partial C_1) = 0. \quad (2.16a)$$

If on the other hand, (2.13a) is used to construct the function $\mathcal{F}$, the branch point condition leads to

$$E_{C_1}^+ + E_{C_2}^+(\partial C_2/\partial C_1) = 0. \quad (2.16b)$$

Finally, elimination of $\partial C_2/\partial C_1$ between (2.16a, b) gives

$$E_{C_1}^+ E_{C_2}^- - E_{C_2}^+ E_{C_1}^- = J_{C_1,C_2}(E^+, E^-) = 0. \quad (2.17)$$

Equation (2.17) may be viewed as a necessary condition for a branch point. Derivatives with respect to C_1 and C_2 are taken by varying the differentiated quantity over different solutions (i.e., over different values of Q, B^- or B^+).

It is also possible to express the equations for the x-structure of the solution in the quasi-linear form (1.4) by substituting the depth and velocity profiles (2.11) and (2.12) into the momentum equation (2.1) and applying the result on both sidewalls along with the boundary conditions (2.8a, b). [The desired form can also be obtained by differentiating (2.13a, b) with respect to x]. In either case the result is

$$\begin{bmatrix} E_{C_1}^+ & E_{C_2}^+ \\ E_{C_1}^- & E_{C_2}^- \end{bmatrix} \begin{bmatrix} C_1 \\ C_2 \end{bmatrix}_x = \begin{bmatrix} -g & -E_w^+ \\ -g & -E_w^- \end{bmatrix} \begin{bmatrix} h \\ w \end{bmatrix}_x. \quad (2.18)$$

Solving (2.18) for (dC_1/dx) leads to

$$dC_1/dx = \frac{g(E^+ - E^-)_{C_2} dh/dx + J_{C_2,w}(E^+, E^-) dw/dx}{J_{C_1,C_2}(E^+, E^-)}. \quad (2.19)$$

The branch point condition $J_{C_1,C_2}(E^+, E^-) = 0$ requires that the numerator in (2.19) vanish in order for dC_1/dx to remain bounded, and this restricts the values dh/dx and dw/dx can take at a branch point. By choosing C_1 and C_2 judiciously this restriction can be further simplified, as shown in the next section.

3. Alternative formulations

It is possible to write down a number of equivalent forms of the equations for the along-stream structure which may be computationally advantageous and provide additional physical intuition. Two such forms result from consideration of the volume flow rate:

$$Q(C_1(x), C_2(x), w(x)) = \int_{-w}^{w} ud\,dy = \tfrac{1}{2} f^{-1} g(D^{-2} - D^{+2}). \quad (3.1)$$

(The second step follows from 2.2). Now (3.1) may be used in place of (2.13a or b) and the steps leading to (2.17) may then be repeated to achieve the required $\mathcal{F}$-function. The resulting branch point conditions are

$$J_{C_1,C_2}(Q, E^+) = 0 \quad (3.2)$$

$$J_{C_1,C_2}(Q, E^-) = 0. \quad (3.3)$$

In connection with these forms, it is convenient to introduce the average wall depth $\bar{D}$ and differential wall depth $\hat{D}$ defined by

$$\bar{D}(x) = \tfrac{1}{2}[D(-w, C_1(x), C_2(x)) + D(w, C_1(x), C_2(x))] \quad (3.4a)$$

$$\hat{D}(x) = \tfrac{1}{2}[D(-w, C_1(x), C_2(x)) - D(w, C_1(x), C_2(x))], \quad (3.4b)$$

in terms of which, the flow rate can be written

$$Q = 2f^{-1} g \hat{D} \bar{D}. \quad (3.5)$$

In principle (3.4a, b) determine C_1 and C_2 in terms of $\hat{D}$ and $\bar{D}$, so that the "constants" in the velocity and depth profiles (2.11) and (2.12) may simply be chosen as $\bar{D}$ and $\hat{D}$. Thus the branch point conditions (3.2) and (3.3) may be written

$$J_{\bar{D},\hat{D}}(Q, E^-) = 2gf^{-1}(E_{\bar{D}}^- \hat{D} - E_{\hat{D}}^- \bar{D}) = 0 \quad (3.6)$$

$$J_{\bar{D},\hat{D}}(Q, E^+) = 2gf^{-1}(E_{\bar{D}}^+ \hat{D} - E_{\hat{D}}^+ \bar{D}) = 0. \quad (3.7)$$

Also note that by substituting $Q/\bar{D}$ for $\hat{D}$ in either (3.6) or (3.7) one obtains a "weir formula"; i.e., one relating the flow rate to the single variable $\hat{D}$ measured at a branch point.

Alternative quasi-linear forms can be written down using the derivative of (3.5) with respect to x along with one of the sidewall momentum equations in (2.18). One such combination is

$$\begin{bmatrix} E_{\bar{D}}^- & E_{\hat{D}}^- \\ \hat{D} & \bar{D} \end{bmatrix} \begin{bmatrix} \bar{D} \\ \hat{D} \end{bmatrix}_x = \begin{bmatrix} -g & -E_w^- \\ 0 & 0 \end{bmatrix} \begin{bmatrix} h \\ w \end{bmatrix}_x, \quad (3.8)$$

and it follows that

$$\bar{D}_x = \frac{-\bar{D}[gdh/dx + E_w^- dw/dx]}{J_{\bar{D},\hat{D}}(Q, E^-)}. \quad (3.9)$$

This expression provides more specific information concerning the channel geometry at the branch point than (2.19) does. For example, when $dw/dx = 0$ the branch point condition $J_{\bar{D},\hat{D}}(Q, E^-) = 0$ requires that the bottom slope vanish ($dh/dx = 0$) or that $\bar{D}$ vanish. The latter would imply that *both* sidewall depths vanish and this condition can usually be dismissed as being unrealistic. If width variations are allowed but the bottom is level then the branch point occurs where $dw/dx = 0$ or where E_w^- and E_w^+ vanish. [The vanishing of E_w^+ follows from the counterpart to Eq. (3.9) obtained when the momentum balance at $y = w$ is used instead of the $y = -w$ balance]. In all known cases, the only situation in which E_w^- and E_w^+ can vanish occurs when the flow separates from one of the sidewalls, and this is discussed more fully in section 5.

Finally we mention a generalized branch point condition due to Stern (1974) and show how it can be derived using Gill's formalism. If the geostrophic relation (2.2) is integrated across the channel, the result can be written

$$\int_{D^-}^{D^+} U^{-1} d(D) + 2fg^{-1}w = 0. \quad (3.10)$$

Now a function of $\mathcal{F}$ can be obtained from the left-hand side of (3.10) by using (2.6) and (2.9) to express u and d in terms of ψ and D^+. After the appropriate substitutions are made and the integration variable is changed from D to ψ, one obtains

$$\mathcal{F}(D^+; h, w) = \int_Q^0 (2fg^{-1}\psi + D^{+2})^{-1/2} \times [2B(\psi) - 2g(2fg^{-1}\psi + D^{+2})^{1/2}]^{-1/2} d\psi - 2w = 0.$$

The critical or branch point condition is now obtained by setting $\partial\mathcal{F}/\partial D^+ = 0$. Doing so and changing the integration variable of the result from ψ to y, one obtains

$$\int_{-w}^{w} (U^2 D)^{-1}[1 - U^2/gD] dy = 0. \quad (3.11)$$

This condition implies that at a branch point the local value of U^2/gD must be unity for some value of $-w < y < w$. Note that the integral in (3.11) can be evaluated in the laboratory if velocity and depth data are available, whereas it is not clear how one would measure the Jacobians in (2.15) or its alternate forms. For computations (such as the examples presented in sections 6 and 7) however, it is often more convenient to use (2.17), (3.2), (3.3) or (3.6).

4. Physical interpretation of the branch point condition

Next consider the physical meaning of the branch point condition (3.6) or (3.7). In the $(\bar{D}, \hat{D})$ plane shown in Fig. 2 we have drawn some Q = constant curves along with some hypothetical E^+ = constant curves. The values of $\bar{D}$ and $\hat{D}$ which occur for different values of x in any given solution must, of course, lie along one of the Q = constant curves. Suppose one follows such a curve and notes the values of E^+ encountered along the way. Since $d\hat{D}/d\bar{D} = -Qf/2g\bar{D}^2 = -\hat{D}/\bar{D}$ along this curve, it follows that

$$dE^+ = E_{\bar{D}}{}^+ d\bar{D} + E_{\hat{D}}{}^+ (d\hat{D}/d\bar{D}) d\bar{D} = \bar{D}^{-1} J_{\bar{D},\hat{D}}(Q, E^+) d\bar{D},$$

and thus E^+ is stationary ($dE^+ = 0$) if the curve passes through a branch point $J_{\bar{D},\hat{D}}(Q, E^+) = 0$. In Fig. 2 the branch point occurs where curves of constant Q and E^+ become parallel, as at the point marked P. Here the value of E^+ is locally extreme with respect to $\bar{D}$ (unless $d^2E^+/\bar{D}^2$ vanishes, in which case P may be an inflection point). In the case of uniform potential vorticity it can be shown that E^+ is a minimum at the branch point. All of these remarks hold for E^- as well.

It is also easy to show that the branch-point condition implies that the flow is critical with respect to a long wave of infinitesimal amplitude. Consider a steady flow containing stationary disturbances which exist independently of any topographic or sidewall forcing. For simplicity we will assume that the channel contains no sidewall contractions or topographic variations (or, equivalently, that the wave length of the wave is much shorter than the scales of variation of w and h). Since the flow is steady the depth and velocity profiles given by (2.11) and (2.12) continue to hold. For stationary disturbances of small amplitude ϵ the x-dependent terms of the solution, $C_1(x)$ and $C_2(x)$, can be expressed as basic parts $\bar{C}_1$ and $\bar{C}_2$ and small departures $\epsilon C_1'(x)$ and $\epsilon C_2'(x)$. Thus the depth and velocity can be expanded in a Taylor series in powers in ϵ as follows:

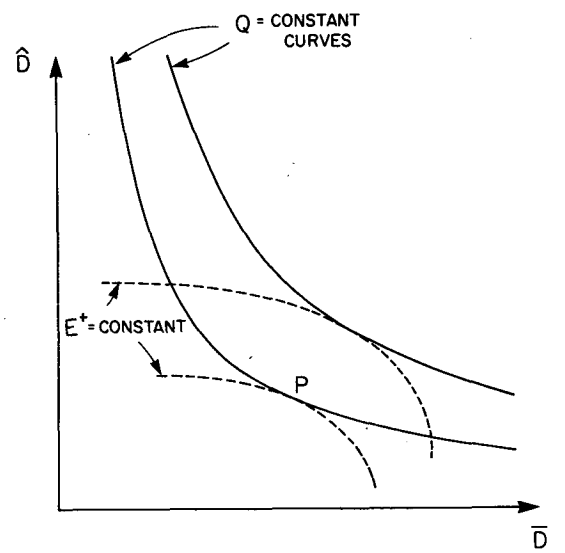

FIG. 2. Curves of constant Q and E^+ in $\bar{D}$, $\hat{D}$ space. Branch points (critical flow) occur where the two families of curves are parallel, as at P.

$$D(y, C_1(x), C_2(x)) = D(y; \bar{C}_1, \bar{C}_2) + \epsilon C_1' \partial D/\partial \bar{C}_1 + \epsilon C_2' \partial D/\partial \bar{C}_2 + \cdots \quad (4.1a)$$

$$U(y; C_1(x), C_2(x)) = -gf^{-1}\partial D/\partial y = U(y; \bar{C}_1, \bar{C}_2) + \epsilon C_1' \partial U/\partial \bar{C}_1 + \epsilon C_2' \partial U/\partial \bar{C}_2 + \cdots. \quad (4.1b)$$

If the x-momentum equation is now evaluated at each sidewall (where $v = 0$) and (4.1a, b) are substituted for u and d, the linearized results are

$$E_{\bar{C}_1}^{+} dC_1'/dx + E_{\bar{C}_2}^{+} dC_2'/dx = 0$$

$$E_{\bar{C}_1}^{-} dC_1'/dx + E_{\bar{C}_2}^{-} dC_2'/dx = 0,$$

where E^+ and E^- are the sidewall specific energies of the basic flow. For a nontrivial x-structure to exist the determinant of the coefficients in the equations for C_1' and C_2' must vanish, leading to

$$J_{\bar{C}_1, \bar{C}_2}(E^+, E^-) = 0. \quad (4.2)$$

Associating the mean flow with a steady flow in a gradually varying channel, the branch condition for the latter is clearly equivalent to the critical condition with respect to a disturbance which does not alter the prescribed potential vorticity.

5. Separated flow

When the velocities in a rotating channel flow become sufficiently large, it is well known that the fluid depth along the wall at $y = w$ can vanish, causing that edge of the current to separate from the wall. The conditions for separation of uniform potential vorticity flow have been discussed by a number of authors, most notably Shen (1981), and examples of separation in laboratory flows have been observed by Whitehead et al. (1974), Shen (1981), and Pratt (1987). We now discuss some general aspects of the hydraulics problem for separated flows with general potential vorticity distributions. To do so, first note that the vanishing of the depth D^+ at the free edge of the current along with conservation of mass [see Eq. (3.1)] require that the wall depth D^- be independent of x. Hence Gill's function $\mathcal{J}$ may be constructed directly from the Bernoulli equation at $y = -w$ [Eq. (2.13b)] in the form

$$\mathcal{J}(U^-; h) = \tfrac{1}{2} U^{-2} + gh = B^- - gD^-. \quad (5.1)$$

Application of (1.2) yields the branch point condition

$$\partial \mathcal{J}/\partial U^- = U^- = 0, \quad (5.2)$$

and therefore the branching of the solution requires that the wall velocity U^- vanish, i.e., a stagnation point occurs.

Differentiation of (5.1) with respect to x yields

$$U^- \partial U^-/\partial x = -g dh/dx, \quad (5.3)$$

and this equation is of the required quasi-linear form (1.4). Note that h_x must be zero when U^- vanishes, so that a branch point must occur at a sill. Thus, a branch point cannot occur at a point of minimum width unless it also so happens that $dh/dx = 0$ at that point. In fact a separated flow is completely insensitive to changes in w, a statement which can be proved as follows. If $dh/dx = 0$, then it follows from (5.3) that U^- is x-independent. Furthermore D^- is x-independent for all separated flows, and it follows from the potential vorticity equation (2.4) that U_y^- is also x-independent. Finally, successive differentiation of (2.4) with respect to y will show that all higher derivatives of U^-, and hence all coefficients in the Taylor expansion of U about $y = -w$, vanish. One consequence of this result is that the flow may not undergo separation in a contracting $dw/dx < 0$ section, with no bottom relief, for its separated width would have to continuously decrease in the downstream direction to avoid reattachment.

It can also be shown that $U^- = 0$ is a critical condition with respect to long waves. To do so, let $C_2(x)$ represent the y-position of the free edge of the current and repeat the calculation culminating in Eq. (4.2). Studies by Stern (1980) and Kubohawa and Hanawa (1984) verify that $U^- = 0$ is in fact the critical condition for separated uniform potential vorticity flow.

The vanishing of the wall velocity at the critical section implies that a recirculation exists with fluid returning upstream (or downstream) along the $y = -w$ wall. Since it is characteristic of steady flows to be subcritical, and therefore have a decreased mean velocity, upstream of the critical section, one might expect U^- to become negative there. The implication is that a return flow exists *upstream* of the control section with a dividing streamline separating this recirculation from the main flow, as shown in Fig. 3. The recirculation may extend indefinitely far upstream of the critical section or may consist of a closed eddy of finite extent. In any case the prespecification of $G(\psi)$ along recirculating streamlines may be invalid; one may be forced to *solve* for $G(\psi)$ in such regions by taking into account friction or other previously neglected processes.

Having discussed the theory, we must note that no example of hydraulically critical, separated flow has been produced in the laboratory. Pratt (1987) induced flow separation in the supercritical flow downstream of a sill by rotating his laboratory channel at a sufficiently high rate, however the critical flow at the sill remained attached for all rotation rates. More revealing are the results of Shen (1981) who also induced supercritical separation, this time downstream of a combination sill and width contraction. As the rotation rate was increased the separation point moved upstream (nearer the critical section) and, at a sufficiently high rotation rate, the separation point reached the critical section and ceased moving upstream. At this rotation rate, agreement between experimental findings and predictions from a zero potential vorticity theory began to break down, and there is some indication of a recirculation region upstream of the control section (Shen, private communication). These findings suggest

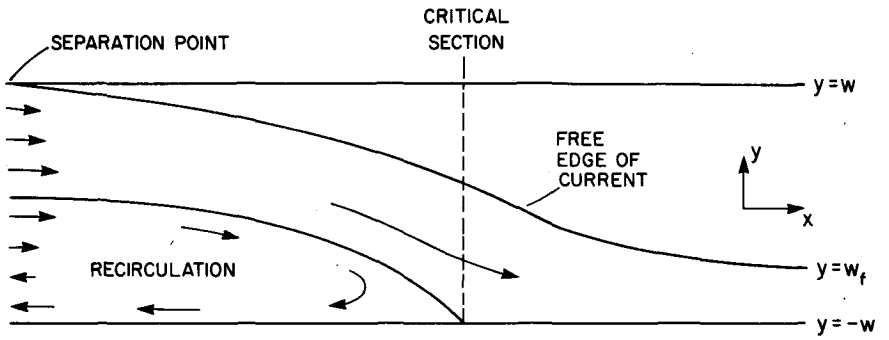

FIG. 3. Anticipated streamline pattern near a critical section when the flow is separated from the wall at $y = w$.

that the recirculating regions, which can arise when flow at a critical section nears separation, undergo potential vorticity modifications which invalidate the theory based on the "original" potential vorticity. This modification may, in fact, prevent separation from occurring at the critical section.

6. Zero potential vorticity example

In this and the following section we present some examples showing the construction of the function $\mathcal{J}$ and the isolation of the critical condition. In the present section we consider several examples of zero potential vorticity flow in order to show that the theory of earlier sections produces the results established by earlier authors.

a. $G(\psi) = 0, f = 0$

When both the potential vorticity and the rotation rate are zero, the depth and velocity become y-independent. This case is the classical hydraulics problem discussed in the textbook of Chow (1959). The Bernoulli and continuity equations (2.6) and (3.1) reduce to

$$\tfrac{1}{2}u^2 + gd + gh = B \tag{6.1}$$

$$2udw = Q. \tag{6.2}$$

Eliminating u between (6.1) and (6.2) leads to the function $\mathcal{J}$ in the form

$$\mathcal{J}(d; h, w) = Q^2/8d^2w^2 + gd + gh, \tag{6.3}$$

and the critical condition $u^2 = gd$ results from setting $\partial\mathcal{J}/\partial d = 0$.

An alternative way of computing the critical condition is to use Eq. (3.3) with $C_1 = d$ and $C_2 = u$, so that

$$U^- = u, \quad D = d, \quad E^- = \tfrac{1}{2}u^2 + gd.$$

Equation (3.3) is thus

$$J_{D,U}(E^-, Q) = 2w(gd - u^2) = 0 \tag{6.4}$$

giving $u^2 = gd$, as before.

b. $G(\psi) = 0, f \neq 0$, nonseparated

If rotation is now allowed, then solving (2.10) with $G = 0$:

$$d_{yy} + f^2g^{-1} = 0 \tag{6.5}$$

yields the depth profile

$$d = \tfrac{1}{2}f^2g^{-1}(w^2 - y^2) - \hat{D}y/w + \bar{D} \tag{6.6}$$

and velocity profile

$$u = -gf^{-1}d_y = fy + g\hat{D}/fw, \tag{6.7}$$

where $\bar{D}(x)$ and $\hat{D}(x)$ are defined by (3.4).

Using (6.6) and (6.7) to evaluate E^- in (2.13b) yields the Bernoulli equation

$$\tfrac{1}{2}(g\hat{D}/fw - fw)^2 + g(\bar{D} + \hat{D}) + gh = B^-. \tag{6.8}$$

The function $\mathcal{J}$ can be constructed by combining (6.8) with the continuity equation (3.5), yielding

$$\mathcal{J}(\hat{D}; h, w) = \tfrac{1}{2}(g\hat{D}/fw - fw)^2 + fQ/2\hat{D} + g\hat{D} + gh. \tag{6.9}$$

The critical condition may be found most easily by applying (3.6), with the result

$$J_{\hat{D},\bar{D}}(Q, E^-) = (g^2\hat{D}^2/f^2w^2 - g\bar{D})2g/f = 0. \tag{6.10}$$

This is the critical condition found by Whitehead et al. (1974) in their study of zero potential vorticity flow through a contraction. The result may also be obtained by setting $\partial\mathcal{J}/\partial\hat{D} = 0$. Further, if one defines

$$\bar{U} = \tfrac{1}{2}[u(w, x) + u(-w, x)] = g\hat{D}/fw,$$

the critical condition (6.10) may be rewritten as

$$\bar{U}^2 = g\bar{D}. \tag{6.11}$$

Hence, the critical condition for the rotating problem may be formed from the nonrotating critical condition $u^2 = gd$ by replacing u and d by their average wall values $\bar{U}$ and $\bar{D}$.

Finally, it can be shown that

$$E_w^+ = -E_w^- = (f^2w^2 - g^2\hat{D}^2/f^2w^2)/w.$$

Recall that the vanishing of E_w^+ and E_w^- is a necessary condition for flow criticality when $dh/dx = 0$ but $dw/dx \neq 0$ [see Eq. (3.9)]. Setting $y = w$, $g\hat{D} = f^2w^2$ and using (6.10) in (6.6) shows that these conditions are also equivalent to the vanishing of the depth at $y = w$. Hence, when $dh/dx = 0$ the flow can become critical at a place other than the narrowest section only by separating from the sidewall, and experimental evidence suggests that this cannot occur.

7. Flow with potential vorticity proportional to the streamfunction

In this section we present an example of a flow with a nonuniform potential vorticity distribution. In order to simplify the problem we only deal here with the case of no background rotation. Despite the fact that $f = 0$, most of the essential physical features of the more general problem are retained, including gravity and potential vorticity waves and vortex stretching by the topography. The only departure from the formalism developed earlier is that here the velocity, rather than depth, serves as the primary dependent variable, a choice necessitated by the fact that $d_y = 0$ when $f = 0$. Finally, the potential vorticity is chosen as

$$G(\psi) = G_0 - a\psi, \tag{7.1}$$

where G_0 is the "background" potential vorticity and a is the potential vorticity gradient.

To obtain an equation for the y-structure of u, we combine the $f = 0$ potential vorticity equation, i.e.,

$$-u_y/d = G(\psi), \tag{7.2}$$

with (7.1) and differentiate the result with respect to y, yielding

$$u_{yy} + ad^2(x)u = 0. \tag{7.3}$$

This equation is used in place of (2.10) to determine the cross-stream structure of the flow.

We will consider the two cases ($a > 0$) and ($a < 0$) separately since they have distinctively different properties. When $a < 0$ the potential vorticity gradient points in the $-y$ direction, as shown in Fig. 4a. Potential vorticity waves presumably propagate to the left of this gradient (i.e., with the flow) so that flow can become critical only with respect to a gravity wave or something akin. In this case one expects the flow to exhibit classical hydraulic behavior. We also note that the Fjörtoft sufficient condition for shear flow stability, (Drazin and Ried, 1981), which in the present case is

$$-uu_{yy} = ad^2(x)u^2 \leq 0, \quad \text{all } -w \leq y \leq w,$$

is satisfied when $a < 0$. When $a > 0$, potential vorticity waves propagate against the flow (Fig. 4b) and the possibility exists for multiple criticalities. In addition, the Rayleigh and Fjörtoft necessary conditions for instability can sometimes be satisfied in this case, a feature discussed later in more detail.

Case 1: ($a < 0$) The solution to (7.3) with $a < 0$ can be written

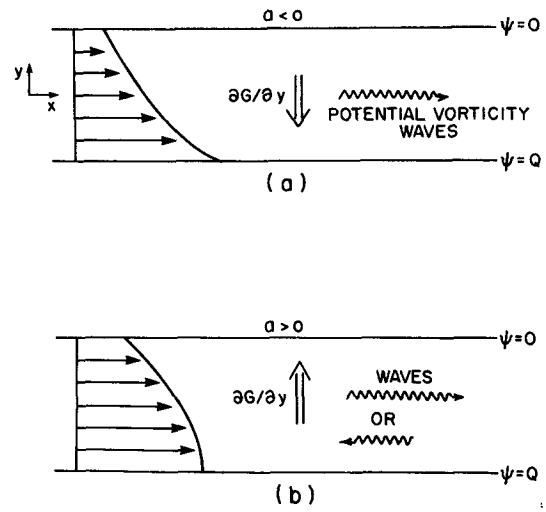

FIG. 4. The direction of the potential vorticity gradient and the anticipated direction of potential vorticity wave propagation when (a) $a < 0$; (b) $a > 0$.

$$u = \frac{\hat{u}\sinh(\alpha y)}{\sinh(\alpha w)} + \frac{\bar{u}\cosh(\alpha y)}{\cosh(\alpha w)}, \tag{7.4}$$

where

$$\alpha(x) = |a|^{1/2}d(x)$$

$$\bar{u}(x) = \frac{1}{2}[u(x, w) + u(x, -w)]$$

$$\hat{u}(x) = \frac{1}{2}[u(x, w) - u(x, -w)].$$

The velocity thus has a boundary layer structure with layers of width α^{-1} along each wall. Since α is proportional to d, the boundary layer width varies in proportion to d^{-1}. In rotating hydraulics with uniform potential vorticity the flow also has a boundary layer structure, however the boundary layer width is fixed by the potential vorticity and therefore cannot vary from section to section (Gill, 1977).

With the definition of the flow rate (3.1), $\hat{u}$ and $\bar{u}$ can be evaluated. Equation (3.1) then becomes

$$Q = \frac{2\bar{u}d}{\alpha}\tanh(\alpha w) = \frac{2\bar{u}}{|a|^{1/2}}\tanh(\alpha w), \tag{7.5}$$

so that

$$\bar{u} = \frac{|a|^{1/2}Q}{2}\coth(\alpha w).$$

At $y = w$, $\psi = 0$ and the potential vorticity equation (7.2) gives

$$-u_y/d = G_0 \quad (y = w),$$

or

$$-\alpha[\hat{u}/\tanh(\alpha w) + \bar{u}\tanh(\alpha w)] = dG_0. \tag{7.6}$$

We can now solve (7.6) with (7.5) for $\hat{u}$ giving

$$\hat{u} = -\tanh(\alpha w)\left(G_0|a|^{-1/2} + \frac{1}{2}|a|^{1/2}Q\right). \tag{7.7}$$

Finally, to obtain Gill's function $\mathcal{F}$ we substitute (7.4) into the Bernoulli equation (2.13b) using the specific energies defined by (2.14b) giving

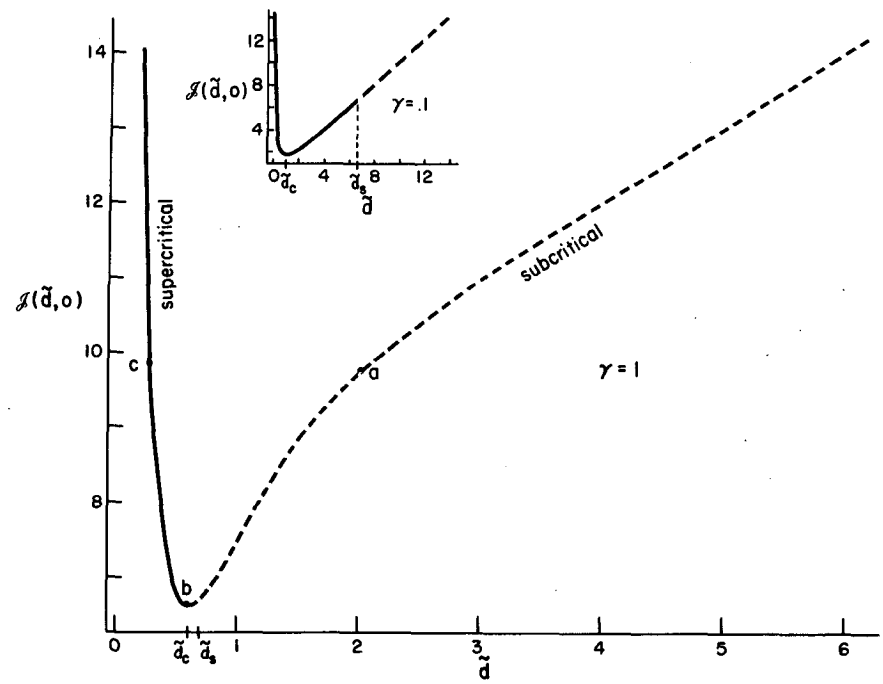

FIG. 5. Plot of $\mathscr{I}$ vs $\tilde{d}$ for the case $a < 0$ with $\beta = 3$, $\gamma = \tilde{Q} = 1$ and $\tilde{h} = 0$. The inset shows a similar plot with $\gamma = 0.1$. Dashed lines indicate that the solution has a velocity reversal.

$$\frac{1}{2}(\bar{u}-\hat{u})^2+gd+gh=B^-,$$

or

$$\frac{1}{2}\left\{\frac{|a|^{1/2}Q}{2\tanh(\alpha w)}+\tanh(\alpha w)(G_0|a|^{-1/2}+\frac{1}{2}|a|^{1/2}Q\right\}^2 + gd+gh=B^-,$$

in view of (7.5) and (7.7). This equation is of the form required by Gill and by nondimensionalizing using gh_m, where h_m is the scale height of the topography, one obtains

$$\mathscr{I}(\tilde{d};\tilde{h})=\frac{\gamma^2\tilde{Q}^2}{2}[1/\tanh(\gamma\tilde{d})+\beta\tanh(\gamma\tilde{d})]^2+\tilde{d}+\tilde{h}, \tag{7.8}$$

where

$$\tilde{Q}\equiv\frac{Q}{2wg^{1/2}h_m^{3/2}}$$

is the dimensionless flow rate,

$$\beta\equiv(2G_0+|a|Q)/|a|Q$$

is the sum of the sidewall potential vorticities divided by the potential vorticity difference,

$$\gamma=|a|^{1/2}wh_m$$

is the channel half width divided by the boundary layer thickness $1/|a|^{1/2}h_m$ based on h_m,

$$\tilde{h}\equiv h/h_m,$$
$$\tilde{d}=d/h_m,$$
$$\tilde{B}^-=B^-/gh_m,$$

and all are nonnegative.

The critical condition can be obtained by setting $\partial\mathscr{I}/\partial\tilde{d}=0$, leading to

$$\gamma^3\tilde{Q}^2[\coth^4(\gamma\tilde{d}_c)-\beta^2]\sinh(\gamma\tilde{d}_c)\operatorname{sech}^3(\gamma\tilde{d}_c)=1, \tag{7.9}$$

where $\tilde{d}_c$ denotes the critical value of $\tilde{d}$. The left-hand side of this expression decreases monotonically as $\tilde{d}$ increases from zero and hence can have only one extremum or branch point. Figure 5 contains a plot of $\mathscr{I}$ vs $\tilde{d}$ for $\tilde{h}=0$, $\beta=3$, and $\gamma=\tilde{Q}=1$ showing a minimum value at $\tilde{d}\approx 0.60$. In dimensional terms (7.9) can be expressed as

$$\bar{u}^2=\hat{u}^2+gh_m\gamma^{-1}\sinh(\gamma\tilde{d}_c)\cosh(\gamma\tilde{d}_c), \tag{7.10}$$

and this reduces to $\bar{u}^2=w^2G_0^2d_c^2+gd_c$ as the potential vorticity gradient vanishes ($\gamma\to 0$). (The classical result $\bar{u}^2=gd_c$ is then obtained by setting $G_0=0$). If $\tilde{d}$ is substituted for $\tilde{d}_c$, it can be shown that the left-hand side of (7.10) is larger than the right-hand side on the left branch of the solution curve in Fig. 5. We therefore interpret the solutions corresponding to this left branch as being supercritical, meaning that long waves propagate downstream. The reverse is true of the right-hand branch and we therefore call the corresponding solutions subcritical. Some caution must be exercised in making this interpretation, however, since we do not

know the actual phase speed of the appropriate long wave away from the control section.

The behavior of the function $\mathcal{F}$ is qualitatively the same as the corresponding functions found in classical or uniform potential vorticity hydraulics. To construct a hydraulically controlled solution for a given topography, $\tilde{h}(x)$, and the parameter settings for the main solution curve in Fig. 5 proceed as follows. First replace the ordinate $\mathcal{F}$ in Fig. 5 by $\tilde{B}^- - \tilde{h}(x)$, giving a plot of $\tilde{B}^- - \tilde{h}(x)$ vs $\tilde{d}$. (This replacement is allowed by the fact that $\mathcal{F}$ was plotted with $\tilde{h} = 0$). Next identify $\tilde{h}_m$, the elevation of highest sill in the prespecified topography. A hydraulically controlled solution will be critical at this sill and the value of $\tilde{B}^-$ for this solution is obtained by equating $\tilde{B}^- - \tilde{h}_m$ with the value of the curve at $\tilde{d} = \tilde{d}_c$ (i.e., the minimum value of $\mathcal{F}$). Values of $\tilde{d}$ for other values of $\tilde{h}(x)$ can be found by locating the point on the curve whose ordinate is $\tilde{B}^- - \tilde{h}(x)$ and choosing the subcritical/supercritical branch upstream/downstream of the sill.

In dimensionless form, the velocity (7.4) can be written

$$\tilde{u} = u/(gh_m)^{1/2}\gamma\tilde{Q} = -\beta\frac{\sinh(\gamma\tilde{d}\tilde{y})}{\cosh(\gamma\tilde{d})} + \frac{\cosh(\gamma\tilde{d}\tilde{y})}{\sinh(\gamma\tilde{d})}, \quad (7.11)$$

where $\tilde{y} = y/w$. Figure 6a shows the velocity profiles of the flow at the points marked a, b and c in Fig. 5. These profiles are representative of the subcritical, critical, and supercritical flow that exist upstream of, at, and downstream of the sill. The profiles have been arranged as they might appear in a channel with constant w and prespecified bottom topography, and a qualitative representation of the depth variation along the channel has been drawn. The most important feature to note is that reverse flow exists along the left-hand ($y = w$) wall beginning slightly upstream of the critical section. At the critical section the flow is unidirectional, so that all of the reverse flow can be traced back along streamlines originating upstream.

To further investigate the conditions under which reverse flow can exist we now search for locations where interior streamlines contact one of the sidewalls. Since the latter can occur only at a stagnation point we set $u = 0$ and $y = w$ in (7.11) resulting in the condition

$$\beta = \coth^2(\gamma\tilde{d}_s), \quad (7.12)$$

where $\tilde{d}_s$ is the depth at the point of separation. The corresponding condition at $y = -w$ is obtained by reversing the sign of the right-hand term in (7.12). Since β is nonnegative this last condition cannot be satisfied and thus streamlines may separate ony from the left wall. "Stagnation" separation should be distinguished from the rotation induced separation discussed earlier in which the wall depth vanishes but u remains finite.

If (7.12) is used to substitute for β in (7.9) the critical condition becomes

$$\gamma^3\tilde{Q}^2[\coth^4(\gamma\tilde{d}_c) - \coth^4(\gamma\tilde{d}_s)] \times \sinh(\gamma\tilde{d}_c)\,\mathrm{sech}^3(\gamma\tilde{d}_c) = 1. \quad (7.13)$$

From this it is clear that $\tilde{d}_c$ must be $<\tilde{d}_s$, and thus streamline separation can occur only in the subcritical flow. In Fig. 5 we have indicated that portion of the subcritical solution branch for which reverse flow occurs by a dashed line. By Taylor expanding $\tilde{d}$ about $\tilde{d}_s$ in (7.13) and using (7.12) it can be shown that

$$\tilde{d}_s - \tilde{d}_c \sim \cosh^4(\gamma\tilde{d}_s)/4\gamma^4\tilde{Q}^2\beta^2. \quad (7.14)$$

For the solution curve in Fig. 5, ($\gamma = Q = 1$, $\tilde{d}_c \approx 0.6$)$\tilde{d}_s - \tilde{d}_c$ is only about 0.05 and thus the separation point lies only slightly upstream of the critical section. The inset in Fig. 5 shows a solution curve for which γ has been reduced by a factor of 10, and here the separation point has been moved well upstream of the critical section.

Case 2: ($a > 0$) The solution to (7.3) for this case is

$$u = \hat{u}\frac{\sin(\alpha y)}{\sin(\alpha w)} + \bar{u}\frac{\cos(\alpha y)}{\cos(\alpha w)}, \quad (7.15)$$

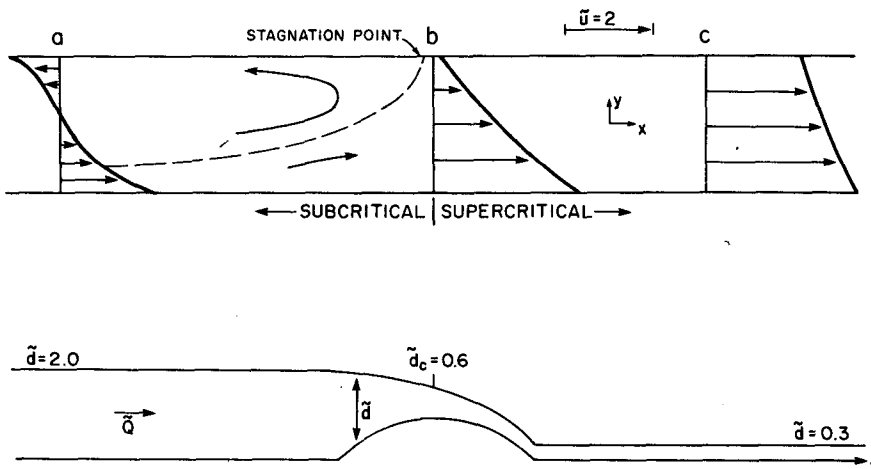

FIG. 6. Qualitative representation of controlled solution based on velocity profiles and depths taken from solution points marked a, b and c in Fig. 5.

where $\hat{u}$, $\bar{u}$ and α are defined as before. The coefficients $\bar{u}$ and $\hat{u}$ can be evaluated using mass flux considerations, as before, resulting in

$$\bar{u} = a^{1/2}Q/2 \tan(\alpha w) \tag{7.16}$$

$$\hat{u} = -\tan(\alpha w)\left[G_0 a^{-1/2} - \frac{1}{2}a^{1/2}Q\right], \tag{7.17}$$

and from these we can form the following dimensionless velocity representation

$$\tilde{u} = \beta\frac{\sin(\gamma\tilde{d}\tilde{y})}{\cos(\gamma\tilde{d})} + \frac{\cos(\gamma\tilde{d}\tilde{y})}{\sin(\gamma\tilde{d})}, \tag{7.18}$$

where $\tilde{d}$, γ, $\tilde{Q}$ and $\tilde{y}$ are defined as before and are nonnegative. Also $\beta = 1 - 2G_0/aQ$ now ranges from $-\infty$ (no potential vorticity gradient) to 1 (infinite potential vorticity gradient). The value $\beta = 0$ occurs when the average potential vorticity

$$\int_0^Q G(\psi)d\psi = -\frac{1}{2}\beta a Q^2$$

vanishes. For $-\infty < \beta < 0$ the average potential vorticity is positive; For $0 < \beta < 1$ it is negative.

The necessary conditions for streamline separation ($\tilde{u} = 0$ at $\tilde{y} = \pm 1$) are now

$$\beta = -\cot^2(\gamma\tilde{d}_s) \quad (\text{at } y = w) \tag{7.19a}$$

$$\beta = \cot^2(\gamma\tilde{d}_s) \quad (\text{at } y = -w). \tag{7.19b}$$

Flow with positive average potential vorticity ($\beta < 0$) can stagnate at the $y = w$ wall only, while negative average potential vorticity flow can stagnate at the $y = -w$ wall only. When $\beta = 0$ stagnation cannot occur for finite $\gamma\tilde{d}$.

Gill's function may be constructed as before through substitution of (7.18) into the sidewall Bernoulli equation (2.13b), resulting in

$$\mathcal{J}(\tilde{d};\tilde{h}) = \frac{1}{2}\gamma^2\tilde{Q}^2[\cot(\gamma\tilde{d}) - \beta\tan(\gamma\tilde{d})]^2 + \tilde{d} + \tilde{h} = \tilde{B}^-. \tag{7.20}$$

Note that $\mathcal{J} \to \infty$ as $\gamma\tilde{d} \to 0, \pi/2, \pi$, etc., so that the curve of $\mathcal{J}$ vs $\tilde{d}$ will consist of an infinite number of lobes, each occupying a depth range of $\pi/2\gamma$. Figure 7 shows $\mathcal{J}(\tilde{d}, 0)$ with the parameter settings $\tilde{Q} = 1$, $\beta = -1$ and $\gamma = 2\pi$. The lobes are numbered $1-\infty$ from left to right. Solutions containing reverse flow are indicated by dashed lines as before.

The critical condition $\partial\mathcal{J}/\partial\tilde{d} = 0$ can be written

$$\gamma^3\tilde{Q}^2[\cot^4(\gamma\tilde{d}_c) - \cot^4(\gamma\tilde{d}_s)]\sin(\gamma\tilde{d}_c)\sec^3(\gamma\tilde{d}_c) = 1, \tag{7.21a}$$

and this equation has infinitely many roots for positive γ and $\tilde{Q}$, one in each interval $0 < \gamma\tilde{d} < \pi/2$, $\pi/2 < \gamma\tilde{d} < \pi$, and so on. Figure 7 shows that the minimum values of $\mathcal{J}$ tend to increase with increasing $\tilde{d}$ and this is due to the potential energy term ($=\tilde{d}$) in (7.20). The asymptotic value of $\tilde{d}_s - \tilde{d}_c$ (for small $\tilde{d}_s - \tilde{d}_c$) can be obtained by replacing $\cosh(\gamma\tilde{d}_s)$ by $\cos(\gamma\tilde{d}_s)$ in (7.14) and from this it follows that $\tilde{d}_s - \tilde{d}_c$ is nonnegative. Thus stagnation will always occur at a greater depth than the critical depth.

The critical condition may also be expressed in the dimensional form

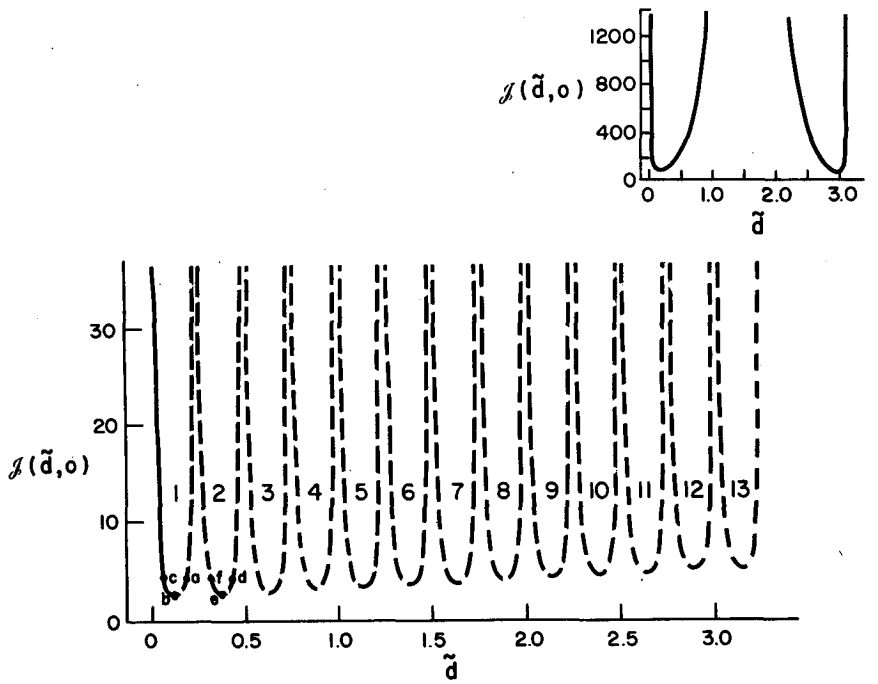

FIG. 7. Plot of $\mathcal{J}$ vs $\tilde{d}$. For case $a > 0$ with $\tilde{Q} = 1$, $\beta = -1$, $\gamma = 2\pi$ and $\tilde{h} = 0$. The inset shows the case $\tilde{Q} = 1$, $\beta = -400$, $\gamma = 1$. Dashed lines indicate that reverse flow exists somewhere over the cross section.

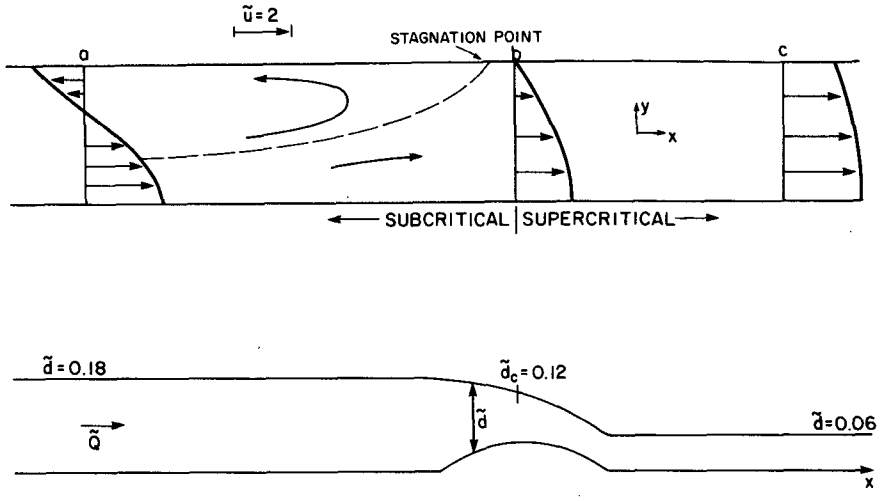

FIG. 8. Qualitative representation of controlled solution from lob #1 of Fig. 7. The velocity profiles and depths are from the points labeled a, b and c in Fig. 7.

$$\bar{u}^2 = \hat{u}^2 + gh_m\gamma^{-1}\sin(\gamma\tilde{d}_c)\cos(\gamma\tilde{d}_c). \quad (7.21b)$$

Consider the relative size of the left and right sides of this expression when $\tilde{d}$ is substituted for $\tilde{d}_c$. For odd-numbered lobes (i.e., $0 < \gamma\tilde{d} < \pi/2$, $\pi < \gamma\tilde{d} < 3\pi/2$, etc.) it can be shown that the left side is larger than the right side on the left-hand solution branches, and we therefore interpret these as representing supercritical solutions. The right-side of (7.21b) dominates on the right-hand branches of odd numbered lobes, and the corresponding solutions are apparently subcritical. On even numbered lobes the reverse is true and the temptation is to label the *right-hand* branches supercritical. However, Eq. (7.16) indicates that $\bar{u}$ is negative for all even lobe solutions, a result that seems to suggest that the flow advects long waves *upstream* (i.e., opposite to the direction of total mass flux). If this interpretation is true, then the right-hand branch solutions would permit wave propagation in the upstream direction only, while left-hand branch solutions would allow propagation in both directions. Due to the apparently unique features of the even lobe solutions, we will not attempt to label the corresponding branches subcritical or supercritical.

Since $\gamma\tilde{d}$ varies over an amount $\pi/2$ within each solution lobe, the velocity profiles have a modal structure particular to each lobe. The higher the lobe number the greater are the number of zero crossings. Figures 8 and 9 contain velocity profiles corresponding to solutions at three points on each of the first two lobes. These points are labeled (a)–(f) in Fig. 7. As before we have arranged the profiles as they might appear in a given physical setting. The lobe 1 profiles (Fig. 8) have been drawn with the subcritical solution (labeled "a" in Fig. 7) followed downstream by the critical solution (labeled "b") followed by the downstream supercritical solution (labeled "c"). Flow at the critical and supercritical sections is unidirectional but a recirculation

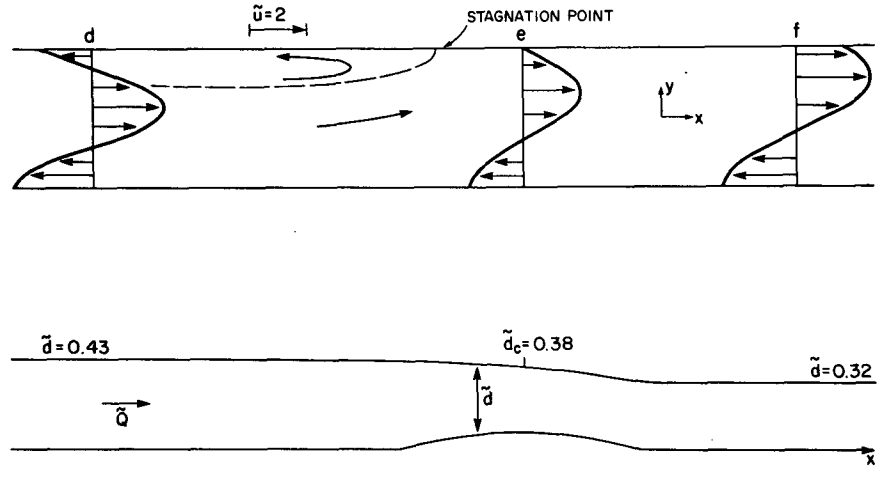

FIG. 9. Lobe 2 solution based upon profiles and depths taken from points d, e and f in Fig. 7.

exists upstream of the critical section. As indicated by Eqs. (7.19) and (7.21) the stagnation point lies on the $y = w$ wall upstream of the critical section. This flow closely resembles the Case 1 solution.

Figure 9 shows the velocity profiles corresponding to points d–f on lobe 2 of Fig. 7. Solution "d" which is hypothesized to support upstream propagation of the controlling wave is placed upstream of the critical solution "e"; solution "f" which apparently supports downstream propagation of the controlling wave, appears downstream. Although the opposite arrangement (solution "d" downstream and solution "f" upstream of the critical section) is dynamically possible, it would support propagation of the controlling wave towards the critical section and thus be unstable (Pratt, 1984b). Hence the correct choice of upstream and downstream solution branches can be made on the basis of stability considerations. The velocity profiles in Fig. 9 contain at most two zero crossings and a recirculation exists upstream of the critical section along the wall at $y = w$, as in the previous case. However, reverse flow now exists along the wall at $y = -w$ and extends over all x. Also note that the relative change in depth across the obstacle is small compared to the previous case.

As the lobe number increases, the effect of topography is reflected more in the vorticity and less in the depth structure of the flow. As a measure of vorticity, consider the cross sectional enstrophy

$$E = \frac{1}{2}\int_{-1}^{1} (\partial\tilde{u}/\partial\tilde{y})^2 d\tilde{y}.$$

Using (7.18) to substitute for $\tilde{u}$ and performing the integration leads to

$$E = \gamma^2\tilde{d}^2(\beta^2 \tan^2(\gamma\tilde{d}) + 1)/2 \sin^2(\gamma\tilde{d}) + \gamma\tilde{d}(\beta^2 \tan^2(\gamma\tilde{d}) - 1)/2 \tan(\gamma\tilde{d}). \quad (7.22)$$

Now consider the change in enstrophy at the critical section $(\partial E/\partial\tilde{d}_c)\Delta\tilde{d}_c$ produced by a small change Δd_c in the critical depth. Such changes might be produced by increasing the topographic height a small amount. Their ratio $\partial E/\partial\tilde{d}_c$ measures the strength of vorticity control relative to depth control. For large $\tilde{d}_c$ we have

$$\partial E/\partial\tilde{d}_c \sim \tilde{d}_c^2/\gamma\tilde{Q}^2 \quad (\text{as } \tilde{d}_c \to \infty),$$

in view of (7.22) and (7.21a). Thus, critical control of depth diminishes relative to enstrophy (or vorticity) control in proportion d_c^2 for large d_c.

When the potential vorticity gradient $(=a)$ is decreased, causing γ and β^{-1} to vanish, the solution lobes begin to separate and eventually all finite values of $\tilde{d}$ are occupied by the first lobe. The inset in Fig. 7 shows the result of decreasing γ to unity and β to -400. The shape of the first lobe is similar to that exhibited by the $\mathcal{F}(\tilde{d}, 0)$ curve of classical hydraulics and the flow is unidirectional over most of the curve. Positive values of β lead to solutions whose general properties resemble those of Fig. 7 except that the stagnation points occur at the opposite sidewall. When $\beta = 0$ no recirculations exist and reverse flows extend over all values of x.

Because multiple solution lobes exist, it is not possible to construct a hydraulically controlled solution in the manner described for the case $a < 0$. Even if the parameters β, $\tilde{Q}$, γ and bottom topography $\tilde{h}$ are prespecified, $\tilde{B}^-$ cannot be determined uniquely; a different value exists for each critical value of $\tilde{d}$. Obviously more information is needed to determine the solution lobe that obtains in a given physical circumstance and one may have to solve a carefully chosen initial value problem to make the correct selection. However, there are a number of features suggesting that the first lobe solution may be preferred in laboratory or geophysical settings. First of all, the lowest-mode solutions are the only ones which do not permit fluid from far downstream to penetrate the control section and are therefore the least objectionable insofar as potential vorticity prespecification is concerned. Furthermore, the critical solution for this lobe has the smallest value of $\mathcal{F}$ and therefore the least energy of all other critical points of all lobes. It follows that a first-lobe solution which is controlled (i.e., has a critical section) possesses the least energy of all other solutions, controlled or otherwise. Should the selection process which establishes steady solutions do so on the basis of minimal energy, the first lobe will be realized. Finally, note that when velocity reversals occur the case $a > 0$ satisfies the Fjörtoft and Rayleigh necessary conditions for instability. (The latter requires that u_{yy} change sign). Although the first-mode solution may be stable, the higher modes are almost certainly barotropically unstable and this again suggests that the first mode may be preferred in natural settings.

8. Discussion

We have established that free flow with nonuniform potential vorticity in a channel of rectangular cross section retains a number of standard hydraulics properties, provided that the potential vorticity is prescribed and that fluid depth remains finite over the entire channel width. Among these are the following:

(i) The flow is symmetric with respect to the channel width and bottom elevation unless the solution passes through a branch point.

(ii) Branch points occur only at topographic "extrema" corresponding to the vanishing of the bracketed terms in Eq. (3.9). For example if the channel width is uniform, branch points can only occur when $dh/dx = 0$, as at a sill. If the bottom elevation is uniform, branch points occur where $dw/dx = 0$, as at a point of minimum width, or where the derivatives of the sidewall specific energies with respect to w vanish. The only known cases in which the latter is satisfied occurs when the fluid separates from one of the channel walls (see example *b* of section 6).

(iii) At a branch point the flow is critical with respect to a long wave which does not disturb the prescribed potential vorticity.

(iv) At a branch point the sidewall specific energies are stationary with respect to changing topography or width. (In all known cases, including the example of section 7, the specific energies achieve extrema at branch points).

Some caution must be exercised in applying these principles, since it may not always be possible to prescribe the potential vorticity on streamlines. One instance where potential vorticity prescription appears to fail occurs when critical flow forms near a point of separation. As discussed in section 5 this type of flow would have a stagnation point at the wetted wall implying a recirculation of fluid upstream or downstream. Recirculations are by no means restricted to flow which experience wall separation due to rotation, as shown by the example of section 7 (in which there is *no* rotation). In any case one may have to solve for (rather than prespecify) the potential vorticity along recirculating stream lines. How to perform this calculation remains an unsolved and important problem. Evidence from recent laboratory experiments suggests that flow at a critical section cannot separate, and this may be a result of potential vorticity modification with recirculations which appear at high rotation rates.

Because a potential vorticity gradient gives rise to many long-wave modes, it is generally possible for flow with given Q, $G(\psi)$ and B^- (or B^+) to have many critical states. In the example of section 7 we showed that an infinite number of critical states were in fact possible. Interestingly enough, each critical state was found to belong to one branching solution pair occupying an exclusive depth range, no two pairs connecting with each other. This isolation may be contrasted with the situation which occurs in sill flow with multiple density layers, where a given solution curve may possess several relative extremums indicating the ability to become critical at different sections (e.g., Farmer and Denton, 1986). Here a solution with predetermined Q, $G(\psi)$, B^-, and "reservoir" depth may become critical only once, unless some sort of hydraulic jump occurs.

Another matter which deserves further attention is the selection of mode number in cases where the $\mathcal{J}$-function has multiple lobes. In the example of section 7, we expressed preference for the lowest mode based on arguments involving potential vorticity prespecification, energy minimization, and stability. However, some consideration of time dependence may be necessary before this question can be resolved.

Acknowledgments. The authors gratefully acknowledge the support of the National Science Foundation (Grants OCE 85-15655 and OCE 83-10889), and the Office of Naval Research (Contracts N00014-85-C-0001 and N00014-85-C-0104). We would also like to thank Mrs. M. Andreasson for typing the manuscript, as well as M. Hall, C. Shen, and the reviewers for their constructive comments.

REFERENCES

Armi, L., 1986: The hydraulics of two flowing layers with different densities. *J. Fluid Mech.*, **163,** 27–58.

Borenäs, K., and P. Lundberg, 1986: Rotating hydraulics of flow in a parabolic channel. *J. Fluid Mech.*, **167,** 309–326.

Chow, V. T., 1959: *Open Channel Hydraulics.* McGraw-Hill, 680 pp.

Drazin, P. G., and W. H. Reid, 1981: *Hydrodynamic Stability.* Cambridge University Press, 527 pp.

Farmer, D. M., and R. A. Denton, 1985: Hydraulic control of flow over the sill in observatory inlet. *J. Geophys. Res. (Oceans),* **90,** 9051–9068.

Gill, A. E., 1977: The hydraulics of rotating-channel flow. *J. Fluid Mech.*, **80,** 641–671.

Hogg, N. G., 1983: Hydraulic control and flow separation in a multilayered fluid with applications to the Vema Channel. *J. Phys. Oceanogr.*, **13,** 695–708.

——, 1985: Multilayer hydraulic control with application to the Alboran Sea circulation. *J. Phys. Oceanogr.*, **15,** 454–466.

Hughes, R. L., 1985: Multiple criticalities in coastal flows. *Dyn. Atmos. Oceans,* **9,** 321–340.

——, 1987: The role of higher shelf modes in coastal hydraulics. *J. Mar. Res.*, **45,** 33–58.

Kubokawa, A., and K. Hanawa, 1984: A theory of semigeostrophic gravity waves and its application to the intrusion of a density current along a coast. Part I. Semigeostrophic gravity waves. *J. Oceanogr. Soc. Japan,* **40,** 247–259.

Pratt, L. J., 1983: On inertial flow over topography, Part I. Semigeostrophic adjustment to an obstacle. *J. Fluid Mech.*, **131,** 195–218.

——, 1984a: On inertial flow over topography. Part 2: Rotating channel flow near the critical-speed. *J. Fluid Mech.*, **145,** 95–110.

——, 1984b: On nonlinear flow with multiple obstructions. *J. Atmos. Sci.*, **41,** 1214–1225.

——, 1986: Hydraulic control of sill flow with bottom friction. *J. Phys. Oceanogr.*, **16,** 1970–1980.

——, 1987: Rotating shocks in a separated laboratory channel flow. *J. Phys. Oceanogr.*, **17,** 483–491.

Roed, L. P., 1980: Curvature effects on hydraulically driven inertial boundary currents. *J. Fluid Mech.*, **96,** 395–412.

Sambuco, E., and J. A. Whitehead, 1976: Hydraulic control by a wide weir in a rotating fluid. *J. Fluid Mech.*, **73,** 521–528.

Shen, C. Y., 1981: The rotating hydraulics of the open-channel flow between two basins. *J. Fluid Mech.*, **112,** 161–188.

Stern, M. E., 1974: Comment on rotating hydraulics. *Geophys. Fluid. Dyn.*, **6,** 127–130.

——, 1980: Geostrophic fronts, bores, breaking and blocking waves. *J. Fluid Mech.*, **99,** 687–703.

Whitehead, J. A., A. Leetmaa and R. A. Knox, 1974: Rotating hydraulics of strait and sill flows. *Geophys. Fluid. Dyn.*, **6,** 101–125.